

Research on the characteristics of the PEP coupling into a metallic via and stub interconnect

XU XIAOFEI^{1,2}, LI DENGHUA^{1,2}, YANG SHUHUI³

¹ School of Electronic and Information Engineering, Beijing Jiaotong University
Beijing, 100044, China

² School of Automation, Beijing Information Science and Technology University
Beijing, 100192, China

³ School of Information Engineering, Communication University of China
Beijing, 100024, China
e-mail: xu18910782910@126.com

(Received: 04.04.2018, revised: 02.07.2018)

Abstract: The research on the coupling electromagnetic effect was studied in this paper, in consideration of the wreaking damage of the powerful electromagnetic pulse to the electronic products. The characteristic of the metallic via and stub interconnect with the coupling voltage was calculated by the model, which was the transfer function $F(f)$ of the protection circuit parameters of DC power source. The research showed that: the smaller radius of Metallic via, the lower amplitude of $F(f)$, the less energy of a power electromagnetic pulse (PEP); the higher increase of the width of the stub interconnect, the bigger reduction of the characteristic impedance of plane wave coupling, the depth of the notch band significantly narrowed. The simulations and experiments were done to compare the protection effects of protection circuits with different parameters at last. The results showed that the protection circuit designed could be highly advantageous in protecting the DC power source in this article.

Key words: powerful electromagnetic pulse (PEP), metallic via, stub interconnect, coupling characteristics, electromagnetic effect

1. Introduction

With the rapid development of the microelectronics technology and high integration of electronic devices, as we all know, we have been left with source cables and other channels of Shielding devices, which have become more and more sensitive to the interference and damage effects of a power electromagnetic pulse [1]. When an external source channel is exposed to a power electromagnetic pulse, it can be coupled or introduced into the interior of electronic devices, spoiling the internal circuit. Therefore, it was of great significance to study the coupling

characteristic of the power electromagnetic pulse and interconnect, where many new innovations of the metallic via and stub interconnect electromagnetic compatibility have been put forward and analysed.

Much of the existing research work was focused on the coupling characteristics of the single frequency plane electromagnetic wave and the opening cavity, and the relationship was calculated between the shielding effectiveness and the electromagnetic wave frequency. However, the real electromagnetic interference was generally caused by the electromagnetic pulse with a certain pulse width, and rich spectrum, such as electrostatic electromagnetic pulses susceptibility, an electromagnetic pulse, lightning electromagnetic pulse and nuclear electromagnetic pulse [2]; the basic principles were studied, which included the transient suppression devices and band-pass filters for suppressing transient large voltage pulses. There were some research focuses on the simulation for PEP coupling with metallic via, with different meshing densities to produce the inaccurate result [3–6].

In this paper, a universal DC voltage strong electromagnetic pulse protection circuit was designed by using the metallic via structure as a transient suppression device and the band-pass filter function of metallic via and stub interconnect as a source channel [7–11]. The via transient suppression components were used to reduce the transient high voltage pulse, and the other band parts of the interference voltage pulse were filtered, and the DC voltage was normally passed to provide the power supply for the subsequent circuit. There were two most important steps in the process: first, the coupling effect of a strong electromagnetic pulse on the line was studied; second, the design of the protection circuit for a DC voltage source was developed. Through simulation and experimental analysis, the protection circuit designed in this paper could protect the DC voltage source from electromagnetic pulse damage to a certain extent.

2. The model design of a metallic via

2.1. The simulation method

In order to solve the mixed simulation problem of a distributed parameter system and a lumped parameter circuit, the finite-difference time-domain-simulation program with integrated circuit emphasis (FDTD-SPICE) simulation method has been put forward [12, 13]. So, the Norton equivalent circuit has been used by mixed simulation of high frequency structure simulation (HFSS), which was based on an electromagnetic field finite element to analyze microwave engineering problems with visualization and a mature adaptive mesh generation technology [14, 15]. The model of an electromagnetic pulse was an incident plane wave approximation, because the general distance to the object in the environment was far away from the electromagnetic pulse source [16].

There was the incident plane wave by approximating from TEM electromagnetic wave irradiation. The central point $A(w_1, l_1)$ was placed at the central position of the outer connection metallic via window, as show in Fig. 1. The dimensions were $a \times b \times c$ of the rectangular cavity, and the x, y, z axes were respectively on the O_{-xyz} . The design method was proposed for on metallic via structure loading open and short stub interconnect object structure, when the ratio of elliptical length to short axis was close to 1.

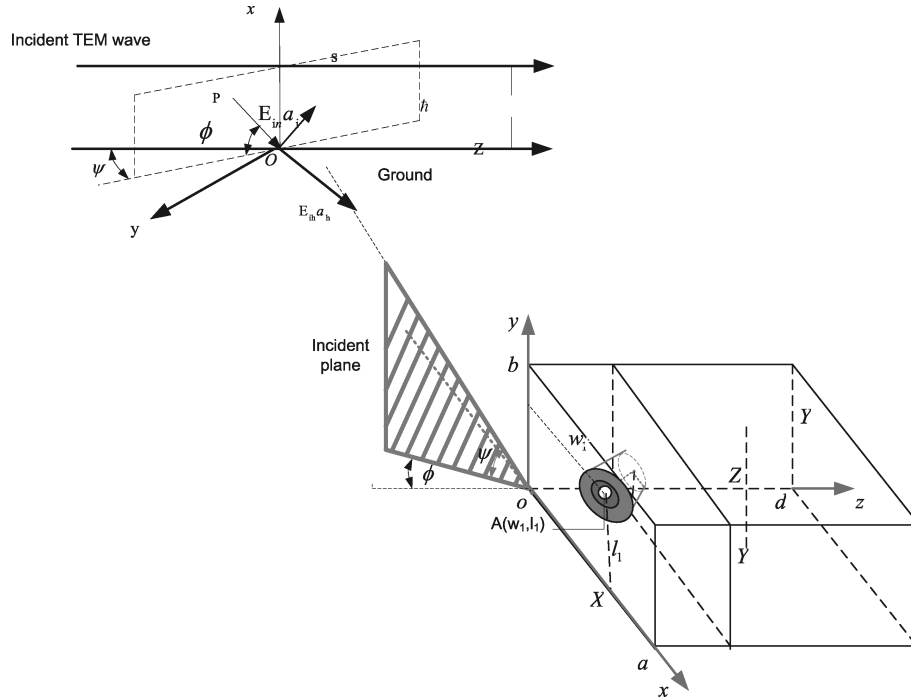


Fig. 1. The system schematic diagram of the plane electromagnetic wave radiation

An incident plane electromagnetic wave was introduced into the input end of a circular cylinder in the modeling. The vertical incidence angle of the plane electromagnetic wave was shown in Fig. 2, the horizontal incidence angle was ψ , and the polarization angle was ϕ , the polarization angle of the electric field was α . Equation (1) was the electric field intensity of the incidence strong electromagnetic pulse.

$$E^{inc} = \begin{bmatrix} (E_0 \cos \alpha \sin \psi \sin \phi - E_0 \sin \alpha \cos \phi) i_x + \\ E_0 \cos \alpha \cos \psi i_y + \\ (E_0 \sin \alpha \sin \phi + E_0 \cos \alpha \sin \psi \cos \phi) i_z \end{bmatrix} \cdot e^{-jk_0 \begin{bmatrix} (\cos \psi \sin \phi) x - \\ (\sin \psi) y + \\ \cos \psi \cos \phi) z \end{bmatrix}}, \quad (1)$$

where i_x, i_y, i_z are the unit vectors in the direction of each axis. As shown in Fig. 2, the circuit model was presented to analyze the field part of the metallic via and stub interconnect terminal load, which was calculated by the FDTD method.

Equation (2) was the scattering voltage $V^{sca}(x)$, which could be represented by the green function, the coupling voltage from the radiation source of the incident plane electromagnetic wave, as show in e.g. (2):

$$V^{sca}(x) = \int_0^L G_V(x; x_s) V_{s2} dx_s - G_V(x; 0) V_1 + G_V(x; L) V_2. \quad (2)$$

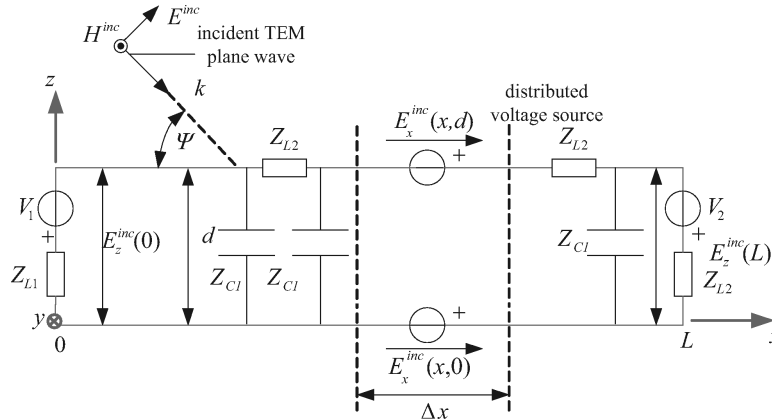


Fig. 2. Transmission line model based on distributed voltage source

Equation (3) was the distributed voltage, as shown in Fig. 2:

$$\begin{aligned}
 V_{s2} &= E_x^{inc}(x, d) - E_x^{inc}(x, 0) = \\
 &= E_0(\cos \alpha \sin \psi \cos \phi + \sin \alpha \sin \phi)(e^{jkd \sin \psi} - 1)e^{-jkx \cos \psi \cos \phi} \approx \\
 &\approx E_0(\cos \alpha \sin \psi \cos \phi + \sin \alpha \sin \phi)jkd \sin \psi e^{-jkx \cos \psi \cos \phi}.
 \end{aligned} \quad (3)$$

Equations (4), (5) represent the interconnect distributed voltage source V_{s2} :

$$V_1 = - \int_0^d E_z^{inc}(0, 0, z) dz \approx -E_z^{inc}(0, 0, 0) d = -E_0 d \cos \psi \cos \alpha, \quad (4)$$

$$\begin{aligned}
 V_2 &= - \int_0^d E_z^{inc}(L, 0, z) dz \approx -E_z^{inc}(L, 0, 0) d = \\
 &= -E_0 d \cos \psi \cos \alpha e^{-jkL \cos \psi \cos \phi} = \\
 &= V_1 e^{-jkL \cos \psi \cos \phi}.
 \end{aligned} \quad (5)$$

In order to describe the coupling effect of copper metallic via and the electromagnetic pulse electric transmission, and Equation (6) was the transfer function $F(f)$. Among them, $U(f)$ was metallic via load terminal voltage, and $E_{inc}(f)$ was the incident electric field intensity.

$$F(f) = 20 \log \frac{U(f)/1}{E_{inc}} = 20 \log \frac{U(f)}{E_{inc} \times 1}. \quad (6)$$

2.2. The simulation model

The effects of an electromagnetic pulse irradiated the metallic via and stub interconnect were studied in the paper. A Gauss pulse is used for the incident electromagnetic pulse (EMP), and its time domain expression is $E(t) = E_0 \exp(-4\pi(t - t_0)^2/\tau^2)$ in the paper; where the function

E_0 was the peak pulse intensity, t_0 was the peak pulse time, τ was pulse width, the appropriate bandwidth was $f = 2/\tau$. The waveform shown in Fig. 3 could reach 38 kv/m of the maximum electric field amplitude.

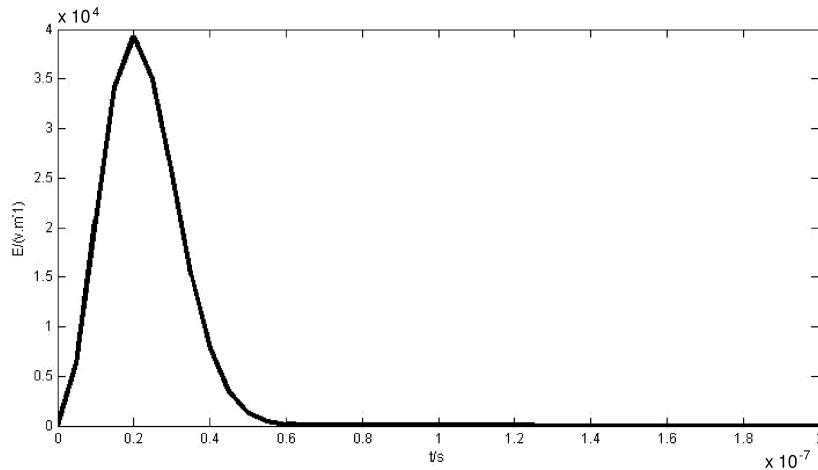


Fig. 3. The waveform of the strong electromagnetic pulse time domain

Electromagnetic pulse energy could be coupled by electromagnetic radiation and transferred in the form of voltage or current; As the FDTD calculation could only simulate a limited space, which was the truncated FDTD grid. Because the truncation of the grid cannot make the obvious reflection of the wave, an absorption boundary condition was set up to absorb the truncated boundary wave from without reflection. When both conditions were met, including the perfectly matched layer (PML, the topside boundary voltage $U = 100v$) method and the metallic via line size smaller than the electromagnetic pulse wavelength, the numerical simulation program has been prepared to find the potential distribution in the coupled metallic via cavity, as shown in Fig. 4(a).

The electrical conductivity of the copper metal material was very large, so the metallic via cavity was set as an ideal conductor. According to the document [11], the cut-off wavelength of the electromagnetic pulse transmitted along the axis was proportional to the radius of the metallic via. The larger the transmission cut-off wavelength, the lower the transmission cut-off frequency, as show in Fig. 4(a). The key was the appropriate selection of the metallic via and stub interconnect lumped impedance or grounding for improving voltage distribution uniformity, the model of which has been presented in Fig. 4(b), r_{gd} was the radius of the gap between the medium substrate, r_0 was the inside radius, r_p was the outer radius, h was the height. When the strong electric magnetic pulse had just started the incident, in the whole shorting stub interconnects experiment condition, the observation of the xOy plane electric field could be seen in Fig. 4(c), which the metallic via was a resistor device with the characteristic of nonlinear volt ampere.

$$C = 1.41\epsilon h \frac{r_p}{r_{gd} - r_p}, \quad (7)$$

$$L = 5.08h \left[\ln \left(\frac{4h}{r_0} \right) + 1 \right]. \quad (8)$$

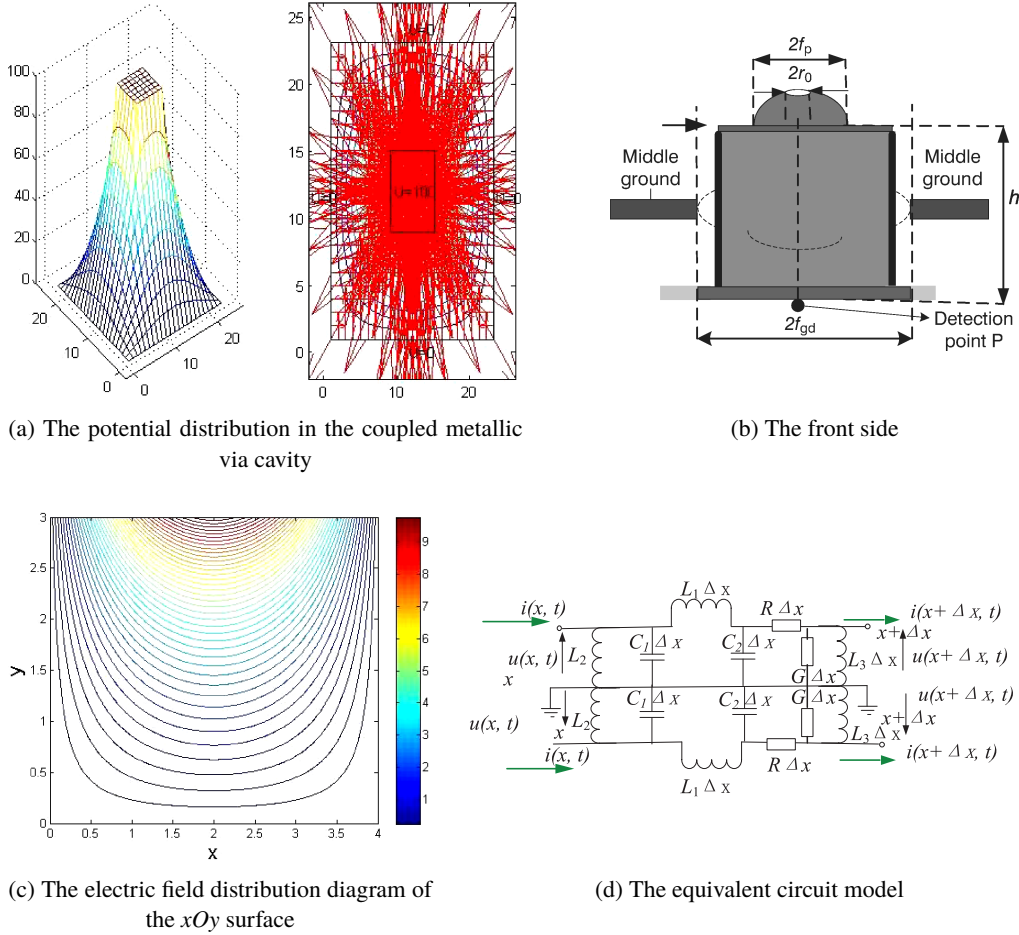


Fig. 4. The model design of metallic via and stub interconnect

Equations (7), (8) were the C, L values, which the Interconnect equivalent capacitance value in the formula could be deduced from Fig. 4(d), that equivalent lumped circuit of metallic via and stub interconnect model.

Next stage, due to the advantages of FDTD in wideband pulse signal and SPICE in complex circuit simulation, the FDTD-SPICE method is used to improve calculation precision and solve efficiency. The inductance value was shown in Fig. 4(d) based on the matched load termination method, as the constraints of Equations (9)–(11) were summarized by Kirchhoff's law.

$$\begin{aligned}
 u(x + \Delta x, t) - u(x, t) &= \Delta u(x, t) = -(R\Delta x)i(x, t) - (L_1\Delta x)\frac{\partial i(x, t)}{\partial t}, \\
 i(x + \Delta x, t) - i(x, t) &= \Delta i(x, t) = -(G\Delta x)u(x + \Delta x, t) - (C_2\Delta x)\frac{\partial u(x + \Delta x, t)}{\partial t}.
 \end{aligned} \tag{9}$$

Getting limit with substitution of equivalence infinitesimal was a common way, then:

$$\begin{aligned}\frac{\partial u(x,t)}{\partial x} &= -Ri(x,t) - L_1 \frac{\partial i(x,t)}{\partial t}, \\ \frac{\partial i(x,t)}{\partial x} &= -Gu(x,t) - C_2 \frac{\partial u(x,t)}{\partial t}.\end{aligned}\quad (10)$$

Then:

$$\begin{aligned}\frac{\partial^2 u(x,t)}{\partial x^2} &= -R \frac{\partial i(x,t)}{\partial x} - L_1 \frac{\partial^2 i(x,t)}{\partial x \partial t}, \\ i(x,t) &= \text{Re} [I(x)e^{j\omega t}], \quad u(x,t) = \text{Re} [V(x)e^{j\omega t}].\end{aligned}\quad (11)$$

3. Numerical results and analyses

3.1. The characteristics of the metallic via of different radius

The incident angle of a strong electromagnetic pulse unchanged under laboratory conditions, the metallic via window radius varied in a certain range, which the coupling effect was observed on PEP and copper metallic via structure from the random sampling vicinity of the upper and lower plane of the cavity, respectively. The characteristic was shown in Fig. 5 of the coupling effects on the metallic via structure parameters, which was analyzed the change of system transfer function caused by dependent variable of the different the opening window radius (r_0 , r_1 , r_2 , r_3 , r_4) of the copper via, as variable relation shown in Equations (7), (8).

Producing a load terminal voltage when the plane incident wave was coupled metallic via cavity. After the scientific data processing, the analysis was shown in Fig. 5: when the opening window radius of the Metallic via was 3.5 mm, the coupling effect was enhanced, which was the consistent with the transmission characteristics from the many papers in reference literature

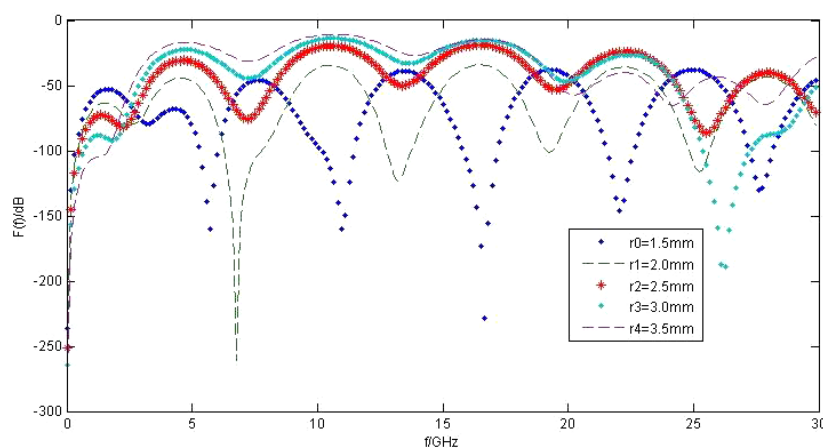


Fig. 5. The characteristics of the different metallic via structure features

list [1]. The radius changed directly with the amplitude of the transfer function, the smaller radius, the lower amplitude, the less energy. There came one of the reasons which a smaller opening window radius leaked the energy of plane incident wave, and the non periodic troughs was caused by the addition of two opposite phase on specific frequency.

3.2. The characteristics of the stub interconnect of different structure features

There remained unchanged about the incident angle of strong electromagnetic pulse and the metallic via window radius, when the stub interconnect structure parameters varied in a certain range, which was observed from the coupling effect between strong electromagnetic pulse and copper metallic via structure in the random sampling vicinity of the upper and lower plane of the cavity, respectively. There were the characteristics on enhancing coupling effects of the stub interconnect structure features, as shown in Fig. 6, which was analyzed the change of system transfer function on enhancing coupling effects of the different stub interconnect structure features, as variable relation shown in Equation (6).

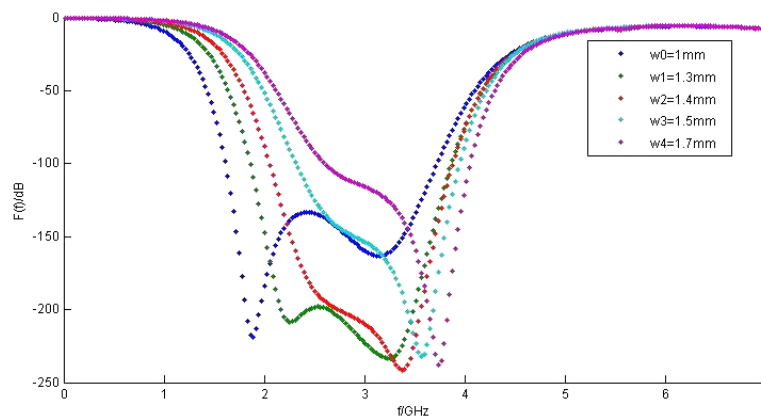


Fig. 6. The characteristics of the different stub interconnect width structure feature

The structure parameters of metallic via loaded stub interconnect was optimized and adjusted, including the length and width of the structure parameters including the positive and negative stub interconnects and short side branches. Producing a load terminal voltage when the plane incident wave was coupled copper metallic via and stub interconnect cavity. After the scientific data processing, the analysis was shown in Fig. 6.

With the width of stub interconnect loaded interconnect increasing ($w_0 \sim w_4$, 1 mm~1.7 mm), the induction voltage amplitude of stub interconnect would decrease first and then increase according to 1 GHz~4.5 GHz bandwidth range. The analysis showed that, due to the increase width of stub interconnect, the characteristic impedance of plane wave coupling was reduced, the depth of the notch band significantly narrowed.

Producing a load terminal voltage when the plane incident wave coupled copper metallic via and stub interconnect cavity. After the scientific data processing, the analysis was shown in Fig. 7. With the length of stub interconnect loaded interconnect increasing ($L_0 \sim L_4$, 5 mm~8 mm), the

induction voltage amplitude of stub interconnect would decrease first and then increase according to 0.8 GHz~3.3 GHz bandwidth range. The analysis showed that, due to the increase length of stub, the characteristic impedance of plane wave coupling was reduced.

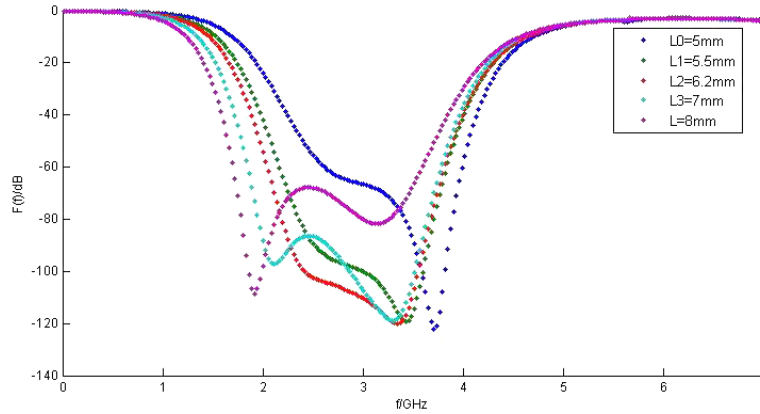


Fig. 7. The characteristics of the different stub interconnect length structure feature

Producing a load terminal voltage, when the plane incident wave coupled copper metallic via and stub interconnect cavity. After the scientific data processing, the analysis was shown in Fig. 8. With the width of stub interconnect loaded interconnect increasing ($w_{d0} \sim w_{d4}$, 0.1 mm~1 mm), the induction voltage amplitude of stub interconnect would decrease first and then increase in 1.5 GHz~4.2 GHz bandwidth range. The analysis showed that, due to the increase width of stub interconnect, the characteristic impedance of plane wave coupling was reduced, the depth of the notch band significantly narrowed; When $w_{d2} = 0.5$ mm, there was transient change, so the appeared places of resonance points and the optimal coupling effect could be adjusted.

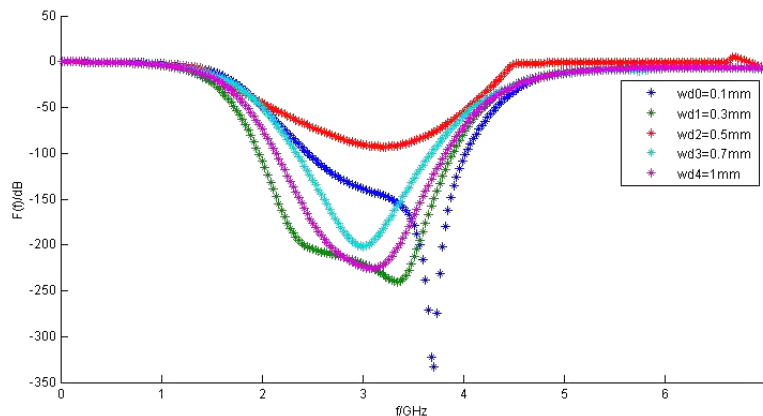


Fig. 8. The characteristics of the stub interconnect different width structure feature

3.3. The resonance characteristics of the metallic via and stub interconnect

The interconnect equivalent capacitance value in the formula could be deduced from Fig. 9, which the computing software has prepared for the metallic via and stub interconnect structural parameter in microwave circuit design; the w_o , w_s were the width, L_s , L_o were the length, h was the height. The important contribution of the paper is finding the optimization parameters that would meet the high-precision machining demand of large aspect ratios between width and height.

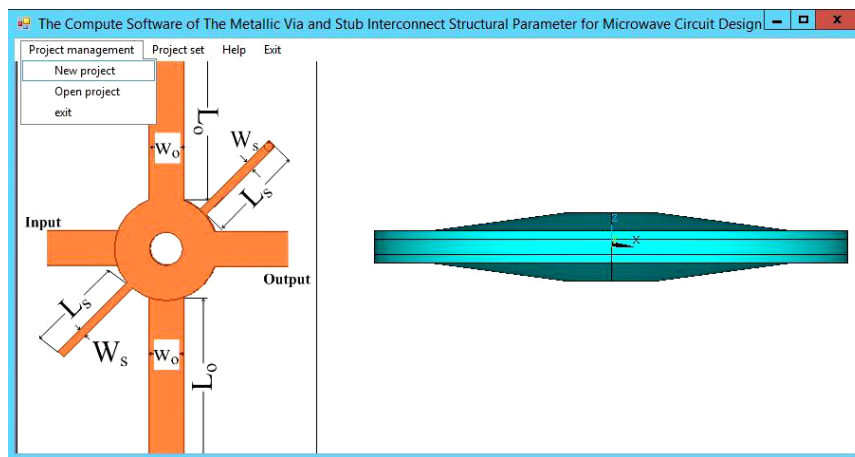


Fig. 9. The computer software of the metallic via and stub interconnect structural parameter for microwave circuit design

It could be seen from Fig. 10, that an electromagnetic inhibition zone was produced in the metallic via cavity.

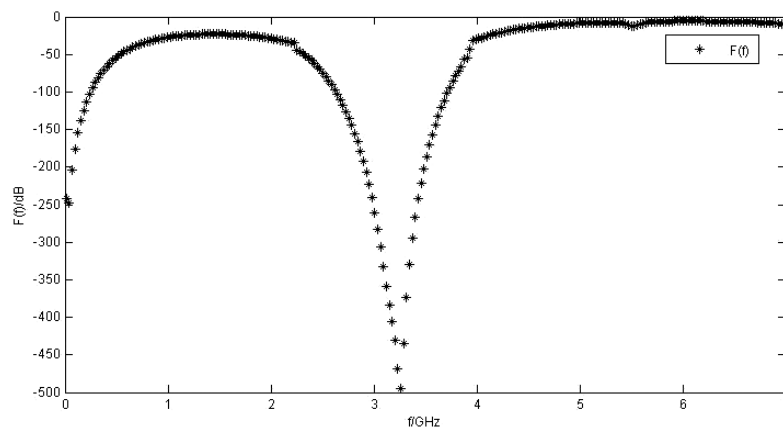


Fig. 10. Filter for actual processing

The simulation showed that the circuit had a good inhibition effect on the high electromagnetic pulse incident wave, and it could protect the DC power within limits. The equivalent circuit structure was the upper and lower mirror symmetric axis of the ground, which could restrain the interference signals by reducing the voltage amplitude of an ultra-wideband electromagnetic pulse and bypassing partial energy of the ultra-wideband electromagnetic pulse.

In the paper, the structural parameters of the metallic via and stub interconnect have been optimized, and there was the simulation result on the performance curve of the transfer function $F(f)$ parameters, as shown in Fig. 10.

There was the inhibition band arrange the center 3.262 GHz in the Fig. 10, and the feedback wave could counteract and reduce the coupling interconnect energy. The amplitude of the customized transfer function decreased, which may be good for the anti-radiation and anti-jamming design to some extent.

There were the optimization parameters of structure, as shown in Table 1.

Table 1. The size of each part of the filter (unit/mm)

W	L	W_s	L_s	W_o	L_o	d	r_{via}	r_p	r_{gd}
5	13	0.4	3	1.7	8	1	0.8	1.6	2.0

Next step, according to the above dimensions, the entity could be fabricated, the FR-4 substrate (thickness 0.9 mm, dielectric constant 4.4), copper foil thickness 0.035 mm, and whole volume size about 30 mm×15 mm×0.9 mm.

4. Conclusions

Based on the analysis of the Metallic via and stub interconnect and its structure model, the paper had studied the characteristic of PEP coupling with the model by using FDTD-SPICE method, which the transfer function characteristic with the coupling voltage was calculated by the model; Then the calculation software was used to make the change and comparison to optimize the structure parameter. So the band-pass filtering made by the Metallic via and stub interconnect could reduce the coupling voltage pulse. It had done a good front job for the follow-up research on electromagnetic pulse protection, and provided a good theoretical basis for engineering practice.

References

- [1] Xu X.-F., Yang S.-H., Li D.-H., Xu Y., *Design of metallic via and stub interconnect loaded band-pass filter*, Journal of Microwaves, vol. 33, no. 6, pp. 38–44 (2017).
- [2] Naredo J.L., Soudack A.C., Marti J.R., *Simulation of transients on transmission lines with corona via the method of characteristics*, IEEE Proceedings Generation, Transmission and Distribution, vol. 142, no. 1, pp. 81–87 (1995).
- [3] Deng J.-Q., Hao C., *Research on Powerful Electromagnetic Pulse Coupling and Power Source Protection*, Journal of microwaves, vol. 33, no. 6, pp. 85–89 (2017).

- [4] Bao Y.-B., Tian Y.-M., Wang C.-X., Wang H.-W., Chen P.-M., *Research on the Characteristics of the NEMP Coupling into a Metallic Cavity with Apertures*, Journal of microwaves, vol. 33, no. 6, pp. 75–80 (2017).
- [5] Gonzalez O., Jose A.P., Herrera A., *An extension of the lumped-network FDTD method to linear two-port lumped circuits*, IEEE Transactions on Microwave Theory and Techniques, vol. 54, no. 7, pp. 3045–3051 (2006).
- [6] Lapohos T., Lovetri J., Seregelyi J., *External field coupling to MTL networks with nonlinear junctions: numerical modeling and experimental validation*, IEEE Transactions on Electromagnetic Compatibility, vol. 42, no. 1, pp. 16–28 (2000).
- [7] Gonzalez O., Jose A.P., Herrera A., *An extension of the lumped-network FDTD method to linear two-port lumped circuits*, IEEE Transactions on Microwave Theory and Techniques, vol. 54, no. 7, pp. 3045–3051 (2006).
- [8] Ndip I., Ohnimus F., Lobbicke K. *et al.*, *Modeling, Quantification and Reduction of the Impact of Uncontrolled Return Currents of Metallic via Transiting Multilayered Packages and Boards*, IEEE Transactions on EMC, vol. 52, no. 2, pp. 421–435 (2010).
- [9] Berenger J.P., *Long range propagation of lightning pulses using the FDTD method*, IEEE Transactions on EMC, vol. 47, no. 4, pp. 1008–1011 (2005).
- [10] Carlos A.F., Sartori J.R.C., *An Analytical-FDTD Method for Near LEMP Calculation*, IEEE Transactions on Magnetics, vol. 36, no. 4, pp. 1631–1634 (2000).
- [11] Lapohos T., Lovetri J., Seregelyi J., *External field coupling to MTL networks with nonlinear junctions: numerical modeling and experimental validation*, IEEE Transactions on Electromagnetic Compatibility, vol. 42, no. 1, pp. 16–28 (2000).
- [12] El-Tanani M.A., Rebeiz G.M., *Corrugated microstrip coupled lines for constant absolute bandwidth tunable filters*, IEEE Transactions on Microwave Theory Tech., vol. 2010, no. 58, pp. 956–963 (2010).
- [13] Berenger J.P., *Perfectly matched layer for the FDTD solution of wave-structure interaction problem*, IEEE Transactions on Antennas Propagate, vol. 44, no. 1, pp. 110–117 (1996).
- [14] Zeng R., Kang P., Zhang B. *et al.*, *Lightning transient performances analysis of substation based on complete transmission line model of power network and grounding systems*, IEEE Transactions on Magnetics, vol. 24, no. 4, pp. 875–878 (2006).
- [15] Dai F., *Scattering and transmission matrix representations of multi-guide junctions*, IEEE Transactions on Microwave Theory and Techniques, vol. 40, no. 7, pp. 1538–1544 (1992).
- [16] Liu X.-H., *Dual-mode Band pass Filter Using Stub interconnect-Loaded Interconnect*, Journal of Radio Engineering, vol. 46, no. 3, pp. 62–64 (2016).